Visual Abstract

Evaluating the safety and the effect of blast loading on the shotcrete together with lattice girder support of tunnels

Hamidreza Karimi Tabar, Farnoosh Basaligheh
Faculty of Civil Engineering, Shahrood University of Technology, Shahrood, Iran
karimitabarhamidreza@gmail.com, f_basaligheb@shahroodut.ac.ir

Majid Nikkhah
Faculty of Mining, Petroleum and Geophysics Engineering, Shahrood University of Technology, Shahrood, Iran
m.nikkhah@shahroodut.ac.ir

ABSTRACT. Damage to tunnels caused by explosions may damage the support structure and the stability. This damage is due to either blasting the working face for drilling progress or an explosion inside the tunnel. The present study investigates the dynamic parameters resulting from the blasting pattern on the temporary support structure of the tunnel considered as a lattice girder and shotcrete equivalent cross-section. For this purpose, LS-DYNA finite element software was used to assess the dynamic response of the structure to the vibration of the blasting-induced explosion. The peak particle velocity (PPV) was considered to evaluate the tunnel's safety under dynamic loads. The results showed that, some levels of destruction would occur by exceeding the velocity of 0.9 m/s in the elements. Regarding the elements of the temporary support structure of the tunnel, it is found that the damage occurs near the face and 2 m from the tunnel.

KEYWORDS. Tunnel, Lining, Numerical modeling, Blasting, Shotcrete.

OPEN ACCESS

Citation: Tabar, H. K., Basaligheh, F., Nikkhah, M., Evaluating the safety and the effect of blast loading on the shotcrete together with lattice girder support of tunnels, Frattura ed Integrità Strutturale, 64 (2023) 121-136.

Received: 27.08.2022
Accepted: 08.12.2022
Online first: 03.02.2023
Published: 01.04.2023

INTRODUCTION

The drilling and blasting method is a conventional and efficient method widely used for constructing underground spaces, especially in tunnels of medium length in civil and mining engineering. Ground vibrations caused by blasting can damage the zones in the vicinity of the explosion and its associated civilian structures. Research on the effects of explosions and blasting loads on underground structures such as tunnels and underground stations has attracted intense interest. Also, some concerns exist about the propagation of the blasting wave and its impact on tunnel's surrounding media, along with the changes in the ground and buried structures. Several numerical studies have been performed on in situ explosions, some of which are represented in the following. There are experimental formulas for predicting ground shocks, both in coupled and non-coupled explosions. Compared to theoretical and experimental studies, numerical modeling is convenient, economical, and relatively accurate for investigating underground explosions, especially in complex cases where experiments are difficult and expensive.

Zhao et al. (1999) studied the dynamic properties of rock materials, the propagation of shock waves in rock masses, and the dynamic response of rock masses and structures. They performed laboratory impact testing on intact rock samples and artificial and natural fractures, field explosion testing, theoretical modeling, and numerical modeling. The results showed that the effects of time and stress waves are two important factors affecting the problems of rock dynamics. These results have been used in the design and construction of the project[1].

Wu et al. (2004) proposed a numerical model for predicting the dynamic response of rock masses to large subsurface explosions. They used the numerical model to predict the dynamic response of the rock mass in terms of particle peak velocity (PPV), particle peak acceleration (PPA), damage area, and frequency content to test the underground explosion. Their results were good consistency with the measured data[2]. Lu et al. assessed the dynamic response of a tunnel structure under surface explosion load. They investigated the time history of displacement, velocity, and pressure parameters in some main points of the subway tunnel in different sections under different conditions, as well as studied the safety assessment of subway structures under surface explosions. Their numerical results showed that the upper part of the tunnel and the center at the bottom of the underground tunnel are susceptible to damage. Moreover, the subway tunnel was found to be safe when exploding 100 kg of TNT at a height of 1.5 m[3]. Mubaraki and Vaghefi (2015) using the finite element (FEM)-based LS-DYNA software, investigated the dynamic response of Kobe subway tunnel (in sandy soil) at depths of 3.5, 7, 10.5, and 14 m under a surface explosion of 1000 kg TNT. The accuracy of the analysis was ensured by comparing, the numerical results with those obtained from the analytical formulas of the US Army Engineering Group (TM-855). Based on the PPV criterion created in the structural elements of the tunnel, the extent of destruction was investigated in different parts and depths of the tunnel[4]. In 2018, Musa et al. assessed the damage of asymmetrical box-shaped underground tunnel explosion based on the PPV and single degree of freedom (SDOF). The results showed slight differences in the above criteria based on the extent of damage to a box-shaped tunnel, under various conditions of explosive load weight and the thickness of the lining at a depth of 4 m. Also, it was found that the efficiency of both methods varies with increasing the tunnel depth. In the PPV method, the tunnel damage is significantly different from the damage level of the tunnel. However, the level of damage obtained through the SDOF technique is largely consistent with the observed tunnel failure modes[5]. Wang et al. (2018) evaluated blasting in the rock masses in a Chinese high-velocity train tunnel. They applied the blasting pattern and well predicted the possible fractures inside the rock and the joints and discontinuities of the rock among the damage contours of numerical modeling. PPV was extracted near the explosion site to estimate the extent and the degree of damage to the surrounding rock mass[6]. Jiang and Zhao (2018) assessed the blasting-caused explosion in the tunnel and its impact on the gas pipe buried in the ground located at a distance from the site of the explosion. The effects of explosion vibration of subway tunnel on the gas pipeline in different tunnel explosion conditions were calculated and the dynamic response characteristics of soil, pipe, and surrounding soil were discussed. Ultimately, to better and more simply investigate and predict the effects of explosion vibration, a PPV prediction model was proposed for this project on a gas pipeline under a subway tunnel drilled through an explosion[7]. Lee et al. in 2018 assessed the internal explosion in China's Chengdu Tunnel. In the research, a severe gas explosion of 2,500 kg of explosive was modeled and the mechanism of structural destruction and the extent of damage in the structure were investigated. The effective stresses and dynamic responses of the lining under explosion impact loading were analyzed. They showed that the highest rate of acceleration and velocity created in the tunnel elements is in its crown while the lowest rate is in its sidewall [8].

A 2D dynamic commercial code was used by Sharafisafa et al. in 2014 to study the pre-splitting blast method. Maximum stresses at halfway between two blastholes in 0.2 ms have been examined for blast loading, blasthole diameter, blast hole spacing ,and joint pattern[9]. Yang et al. (2015) simulated numerical rock mass damage in deep tunnel excavation through the blasting method and assessed the damaged area. Modeling was performed using the LS DYNA software. These authors focused was on the combined effects of stress redistribution resulting from successive explosions in the surrounding rock masses and the resulting damage [10]. In another study, Zhao et al. 2016 experimentally and numerically investigated the effect of vibration caused by an explosion from a nearby tunnel. They performed field monitoring to investigate the effect of explosion vibration from an adjacent tunnel on an existing tunnel. They used the FEM to assess the explosion vibration velocity and vibration frequency of the existing tunnel. The results showed that field monitoring and numerical simulation could optimize the explosion and act as a reference for other similar engineering projects[11]. Ozacar et al.(2018) analysis has been carried out by a new methodology in minimizing the blast-induced ground vibrations at the target location[12]. F Lie et al.(2019) explores the effects of fragmentation of different decks detonated simultaneously in a single borehole with the use of numerical analysis. As expected, the near-borehole area was damaged by compression stresses, while far zones and the free surface of the boundary were subjected to tensile damage[13]. Guan et al. (2020) investigated the velocity, stress response, and damage mechanism of three types of pipelines under vibration explosions in a highway tunnel. They showed that the rate of increase in stress in the pipeline was quite greater than the

induced velocity. Moreover, there was no consistency between the peak velocity position and the maximum stress position[14]. Chamanzad et al.(2020) work is to investigate the effects of the geomechanical and geometrical parameters of rock and discontinuities on the rock mass blasting using the UDEC software. The results obtained show that the joint parameters and rock modulus have very significant effects, while the rock density has less a effect on the rock mass blasting[15]. Dimitraki et al. (2021) developed a finite element code by applying the Jones-Wilkins-Lee (JWL) equation to describe the thermodynamic state of simulating the rock blasting process. A progressive damage model was also used in order to define the stiffness degradation and destruction of the rock material[16].
In this paper, we investigate the dynamic parameters obtained from the explosion of the blasting pattern on the temporary tunnel support structure, which is often the Shotcrete together with lattice girder support. the structure's dynamic response to the explosion vibration caused by blasting was investigated using the FEM-based LS-DYNA software. Here, the PPV criterion was considered to evaluate the tunnel's safety under dynamic loads. Blasting was modeled thoroughly on a full scale and simulations were conducted for rock media, tunnel structure, explosive, stemming, and air inside the tunnel.
Eventually, the present study can be extended to the blasting patterns which are used for drilling in different rock types.

NUMERICAL MODELING

Geometry and characteristics of the model

The structure of the D-shaped cross-section tunnel was investigated along with numerical analysis of the surrounding environment, the rock mass, and the load caused by the charging explosives into holes drilled in the rock. Moreover, the dynamic response of the temporary support structure, shotcrete together with lattice girder, with dimensions of 4 m × 5 m and an overburden of 1.7 m was studied numerically. The Fluid-Structural Interaction (FSI) was created in the numerical simulation. The elements were of SOLID type. The numerical method was validated using, experimental relations to control the data in the elements and confirm the results. Figs. 1 and 2 represent the geometric characteristics of the modeled environment and the used blasting pattern, respectively. According to Fig. 1, modeling was in full scale with the dimensions of 10 m × 8 m × 6.5 m. The rock material elements, the tunnel support structure, the air, the explosive, and the stemming all are in the form of a SOLID quadrilateral. The SOLID elements are the most common method in explicit analysis, where each element is connected to the other element by eight nodes. Fig. 2 represents the arrangement of blast-holes and their delay time based on their location. The diameter of the drilling holes is 5 cm and their depth is 2 m, of which 1.5 m from the end is for charging explosives into holes and 0.5 m from the beginning is for stemming.

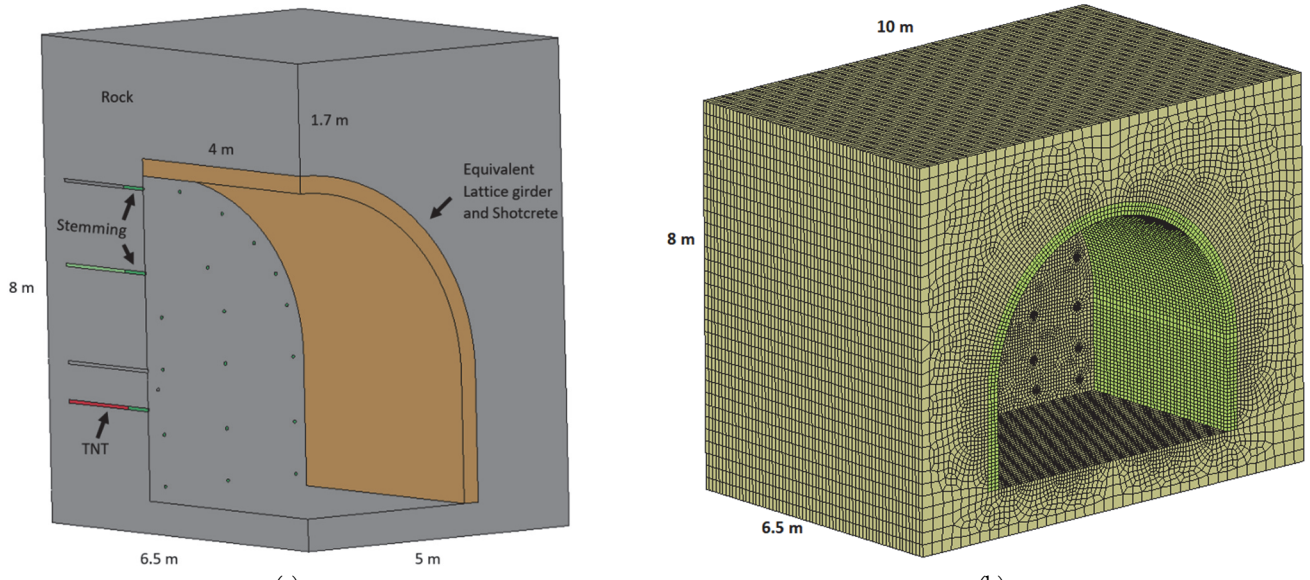

(a) (b)

Figure 1: The geometric characteristics of the model.

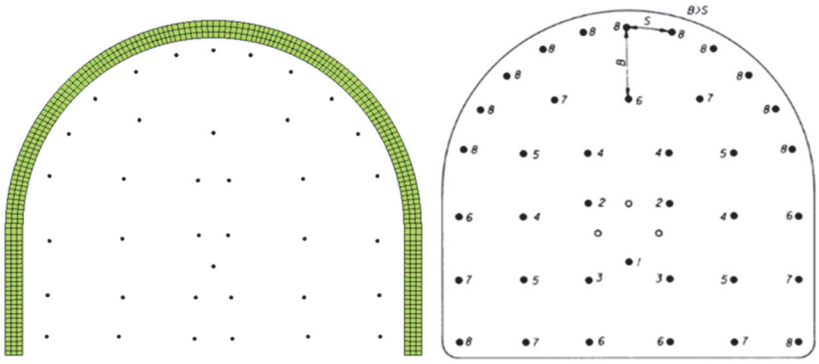

Figure 2: The blasting pattern.

Material model: Air

Numerical modeling of air with material 9 was performed using MAT_NULL software and EOS_PLOYNOMIAL_LINEAR mode formula (Eq. 1&2)[4]. In Eq. (1), the internal energy units of volume, E, and pressure, P, are linear, as follows:

$$P = C_0 + C_1\mu + C_2\mu^2 + C_3\mu^2 + (C_4 + C_5\mu + C_6\mu^2)E_0 \quad (1)$$

and

$$\mu = \frac{\rho}{\rho_0} - 1 \quad (2)$$

where, C0, C1, C2, C3, C4, C5, and C6 are the constants of the equation, ρ/ρ0 is the density ratio, and E0 is the internal energy per unit volume. Tab. 1 represents the parameters for air considered in numerical modeling [4].

V0	E0 (MPa)	C6	C5	C4	C3	C2	C1	C0	ρ (kg/m³)
1	0.25	0	0.4	0.4	0	0	0	0	1.29

Table 1: The characteristics of air in numerical modeling [4].

Material model: The equivalent cross-section of shotcrete and lattice girder

The thickness of the Shotcrete was 27 cm. Also, considering the 1-m spacing of lattices from each other and the equivalent thickness, the thickness still is 27 cm when using 3-rebar lattices. The specifications of the material used for this purpose are presented in Tab. 2 [17]. The modeling was done using the MAT-Plastic-Kinematic and based on the principle of equivalent stiffness, which is widely used in simulations.

Failure strain	Hardening parameter	Tangent Modulus (GPa)	Yield Stress (MPa)	υ	E (GPa)	ρ (kg/m³)
0.8	0.5	4	100	0.25	25.17	2650

Table 2: The properties of the cross-sectional material model equivalent to lattice girder and shotcrete [17].

Material model: Explosive

The TNT charge is modeled by MAT_HIGH_EXPLOSIVE_BURN. Tab. 3 presents the related parameters. The JWL mode equation is utilized extensively in engineering calculations for modeling explosion pressure. This equation of state is written as Eqn. 3.

$$P = A\left(1-\frac{\omega}{R_1 V}\right)e^{-R_1 V} + B\left(1-\frac{\omega}{R_2 V}\right)e^{-R_2 V} + \frac{\omega E_0}{V} \quad (3)$$

where P is the pressure, V represents the ratio of the current volume to the initial volume, and E is the initial energy. This state equation is commonly utilized to describe the behavior of explosion products. It also represents the relationship between pressure, variable volume, and internal energy. A, B, R1, R2, and ω are the constants of specific explosives[18].

B (MPa)	A (MPa)	P_{cut} (MPa)	V_D (m/s)	ρ (kg/m^3)
3.747E3	3.738E5	2.1E4	6930	1630
E_0 (MPa)	V_0	ω	R_2	R_1
6E3	1	0.35	0.9	4.15

Table 3: The properties of explosive model [20].

Material model: Rock mass

The physical and mechanical characteristics of the rock mass surrounding the tunnel are presented in Tab. 4. Considering the main goal of the present research, the material model MAT_MOHR_COULOMB was used as an ideal elastic-plastic material [20]. The specifications of rock mass materials of the environment around the tunnel are presented in Tab. 4. These values are in the weak category in terms of rock mass quality. Hence, it is essential to use the lattice girder and Shotcrete for support and stability of the tunnel.

Lateral Earth Pressure Coefficient	Friction Angle (degree)	Cohesion (kPa)	υ	E (GPa)	ρ (kg/m^3)
0.54	30	200	0.35	0.5	2200

Table 4: The characteristics of rock mass materials surrounding the tunnel [20].

Material model: Stemming

For stemming the explosive holes, the material model MAT_SOIL_AND_FOAM was used, for which the characteristics are presented in Tab. 5. Here ϱ is the mass density, G is the shear modulus, K_U is the bulk modulus [4].

P_{cut} (MPa)	a2	a1	a0	Ku (MPa)	G (MPa)	ρ (kg/m^3)
0	0.87	0	0	5.51	1.72	1255

Table 5: The characteristics of stemming material model [4].

Numerical analysis

An Arbitrary Lagrangian-Eulerian (ALE) solver is used to analyze the finite element model. This method can present the best properties of pure Lagrangian and Eulerian solvers because of the unique motion of the nodes during the analysis. During the analysis, since the nodes can remain constant within an Euler formula, or move with the material like a Lagrangian formula; in the ALE analysis method, they move as the combination of two formulas. ALE can solve the

problems related to more mesh deformation and provide higher clarity than the other methods. The ALE method allows the modeling of fluid-structure interaction (FSI) with the fluid-structure connection algorithm satisfying the existing governing equations, mass, motion, and energy conservation[19].
In the present study, the Lagrangian method was utilized to model the equivalent cross-section of the temporary tunnel structure. The ALE method was also used to model air, rock, explosives, and stemming. Lagrangian and Eulerian nodes are connected using the keyword CONSTRANED_LAGRANGE_IN_SOLID[20]. Using this keyword necessitates the nodes of Lagrangian and Eulerian nodes to overlap with each other. To not stop the analysis process and prevent severe distortions of the Lagrangian section including the equivalent cross-section of the temporary structure, the model of air material was used in the tunnel environment to create the necessary overlap. Moreover, considering the conducted modeling, the CONTACT section and the AUTOMATIC_SURFACE_TO_SURFACE option were used for the contact surface between the tunnel structure and the surrounding rock media[21].

RESULTS AND DISCUSSION

Validation

The developed damage model was validated by comparing the numerical results and those from the empirical relations.

Validation: Air

Considering the amount of explosives under study, it is practically impossible to verify the explosive in the real environment. Hence, it was investigated according to the existing empirical relations. Since the blast wave is also transmitted from the air, the empirical relationship developed by Henrich et al. was utilized to ensure the accuracy of the modeling [22]. They achieved the maximum explosion-caused pressure in the scaled distance (Z), as follows; In Eqs. (4) and (5), ΔP_f is the maximum overpressure caused by the blast wave, Z represents the scaled distance, R is the distance from the explosion site in m, and W is the explosion rate in kg. Explosive cost modeling in the air was performed and compared with experimental relationships to validate the obtained values of the results. The results were validated by running the explosive modeling in the air and comparing the results with those of the experimental relationships. The air model was a cube with dimensions of 3 m, for which the explosive of 100 kg of TNT was applied. Fig. 3.a represents the results of numerical modeling and the experimental relationship at the measurement points. As seen, there is an acceptable consistency between numerical modeling results and the experimental relationship in terms of values and the trend of changes. Therefore, the accuracy of the numerical modeling of the explosion load is confirmed. Fig. 3.b represents the measurement points with specified distances from the explosion site. These distances were based on the amount of explosives in Eq. (4) along with scaled distance. The amount of pressure is presented in Fig. 3.a.

$$\Delta P_f = \begin{cases} \dfrac{1.40717}{Z} + \dfrac{0.55397}{Z^2} - \dfrac{0.03572}{Z^3} + \dfrac{0.000625}{Z^4} & 0.05 \le Z \le 0.3 \\ \dfrac{0.61938}{Z} - \dfrac{0.03262}{Z^2} + \dfrac{0.21324}{Z^3} & 0.3 \le Z \le 1 \\ \dfrac{0.0662}{Z} + \dfrac{0.405}{Z^2} + \dfrac{0.3288}{Z^3} & 1 \le Z \le 10 \end{cases} \quad (4)$$

and

$$Z = \frac{R}{\sqrt[3]{W}} \quad (5)$$

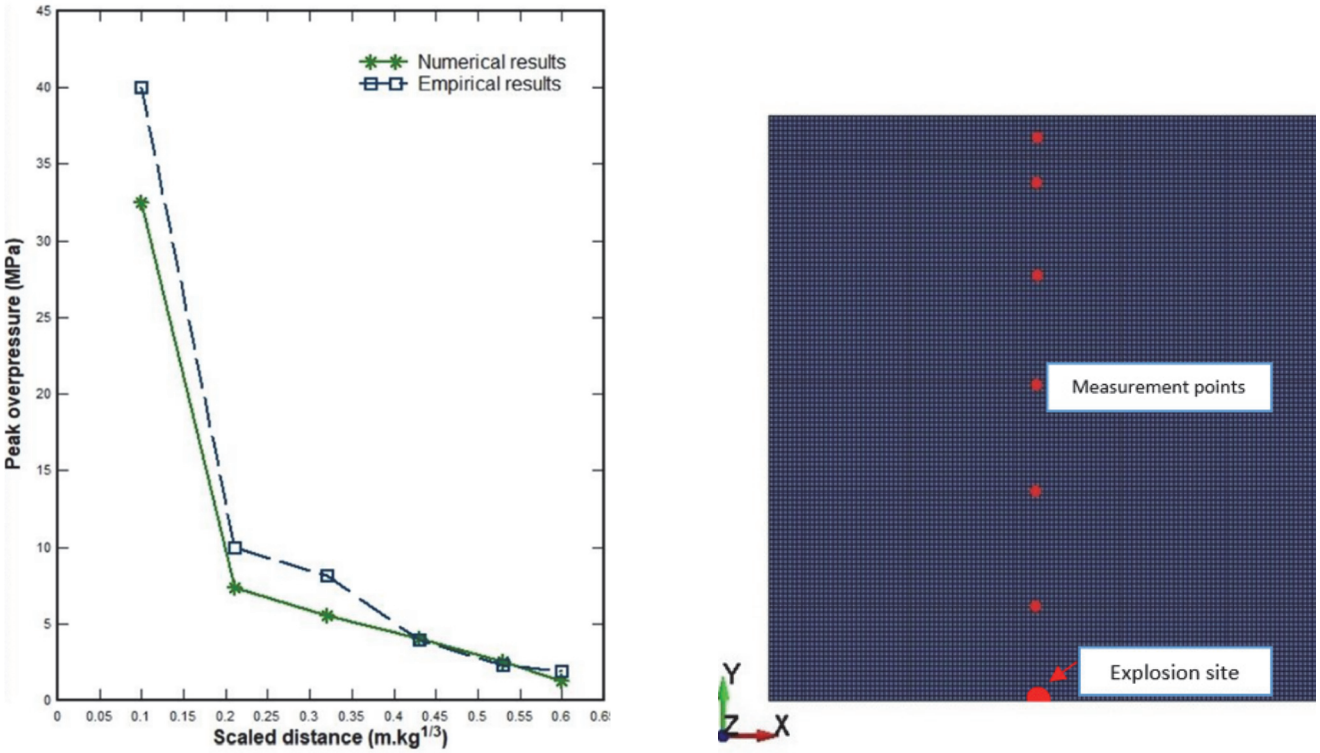

(a) (b)

Figure 3: (a) The comparison of numerical modeling results and experimental results and (b) The location of measuring points.

Validation: Rock mass

The numerical simulation of the effects of the explosion vibration on the tunnel was performed based on the study of Nanjiang et al. (2012). Then, vibration velocity generated in the surrounding rock was analyzed at different positions based on field experiments and the site of the explosion[23]. Tab. 6 presents the comparison of the results of modeling and measurements. According to Tab. 6, the difference between the numerical modeling and the velocities measured by the device is 13% on average indicating a lower modeling error.

Percentage Difference (%)	Velocity from Modeling (cm/s)	Measured Velocity (cm/s)	Distance (m)	Explosive (kg)
10.88	1.5	1.683	69.7	45
10.7	1.81	1.634	61.2	33
5.05	1.62	1.542	63.9	32
14.4	2.19	1.919	50.9	32
25.8	1.27	1.009	62	25.8

Table 6: The comparison of experimental relationship and numerical modeling of rocks.

Parametric studies

This section reviews the results of the numerical analysis of LS-DYNA software on the cross-sectional support structure equivalent to Lattice girder and shotcrete. The simulated velocity and acceleration results were investigated at the desired points, as it is shown in Fig.4**.** Five groups of measurement points from A to E of the tunnel structure are presented in Fig. 4 in order to study the dynamic parameters. Each group includes five measurement points with a distance of 0.50m between them, with the first point closest to the site of the explosion (e.g.A1) and the farthest point (e.g. A5) 2m away from the working face. The same procedure was applied to points B, C, D, and E. Points A to E are from the tunnel crown to the lowest point of the tunnel sidewall.

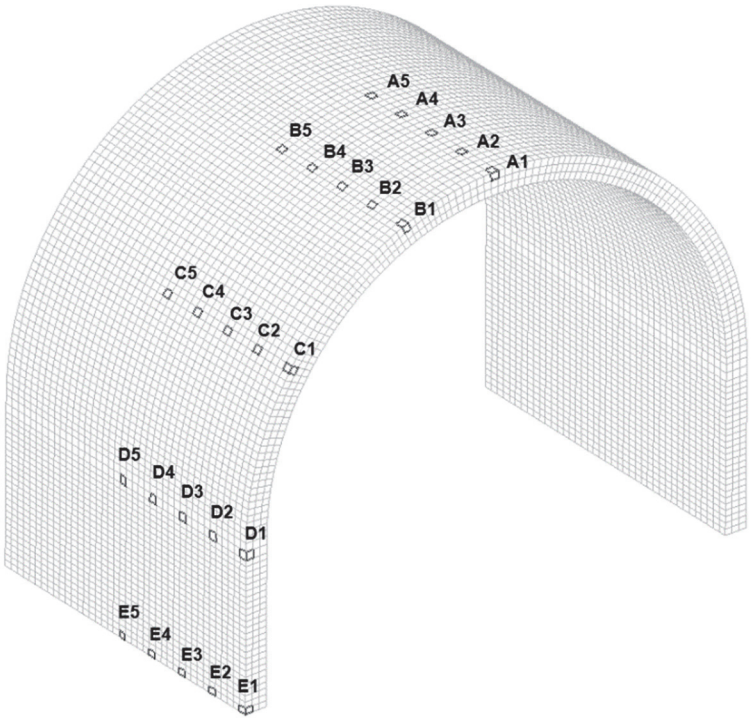

Figure 4: The points studied in the cross-section equivalent to lattice girder and shotcrete.

Parametric studies: Propagation of effective stress around the hole

Von mises effective stress is considered as the non-axial equivalent for the multiaxial in several destruction and yield criteria. Hence, if the material is destructed in a non-axial pressure test ($\sigma 1$ is the only non-zero stress component), by $\sigma 1 = \sigma crit$, the considered structure will also be degraded at multi-axis loads[24]. According to the blasting pattern in Fig 2, the explosion process is initiated at the points of the holes with a time difference of 1 ms. Effective stress is a force holding the particles rigidly together. It simply changes by applying additional forces. Fig. 5 shows the contour of the effective stress propagation resultant from the explosive loads originating from the delay of the blasting pattern created around the blast. It is observed that after initiating the explosion at zero seconds, the blast wave propagates spherically in the rock around the holes. Each blast wave overlaps and interferes with its subsequent blast wave. It is attenuated over time by moving away from the blast site, hence reducing the maximum stress.

Parametric studies: Velocity motion parameter

As mentioned, several sign points (Fig. 4) were investigated at different distances and positions from the tunnel face to assess the effect of blasting and explosion on the tunnel face. The factors considered for this purpose are the defined explosion pattern on the temporary support structure. As seen in Fig. 6.a, the PPV varies from Points A1 to A5. The reduction trend of vibration velocity is also different for points A1 to A5. This difference indicates that point A1 receives more energy from the blast wave than point A5 similar to other points.

The peak velocity at Point A1 is 2.15 m/s, and 1.75, 1.65, 1.57, and 1.52 m/s at Points A2 to A5, respectively. It is observed that the peak velocity created in the structural elements from Point 2 to Point 5 is attenuated compared to point 1. It decreases by 19%, 24%, 27%, and 30%, respectively. In the range of B, the peak velocity in the element reaches 2.8 m/s at Point B1. Moreover, the peak velocity resultant from the second wave generated at point B1 is approximately equal to its maximum at Point B2. It is observed that the reduction rate of velocity at Points B3, B4, and B5 is not significant. Also, at points, C2 to C5 (Fig. 6.c), a reduction of 40%, 48%, 50% ,and 52% is observed compared to Point C1. In Fig.6.d, the peak velocity (PPV) is 1.45, 0.75, 0.65, 0.62, 0.6 m/s at Points D1-D5. In the range of D, since the nearby explosive hole explodes in 5 ms, the peak velocity occurs in 6 ms. However, in other ranges (A, B, C, E), the peak value occurs in 8 ms. Fig.6.e represents PPV for Points E1-E5.

The peak velocity in element E1 is 2.6 m/s and the reduction rate of velocity is 31%, 52%, 62%, and 70% in elements E2 to E5, respectively, compared to element E1. Therefore, the blast wave is attenuated while losing its energy, and the velocity decreases along with the tunnel structure. Fig. 7 displays the velocity contour of the tunnel support structural element.

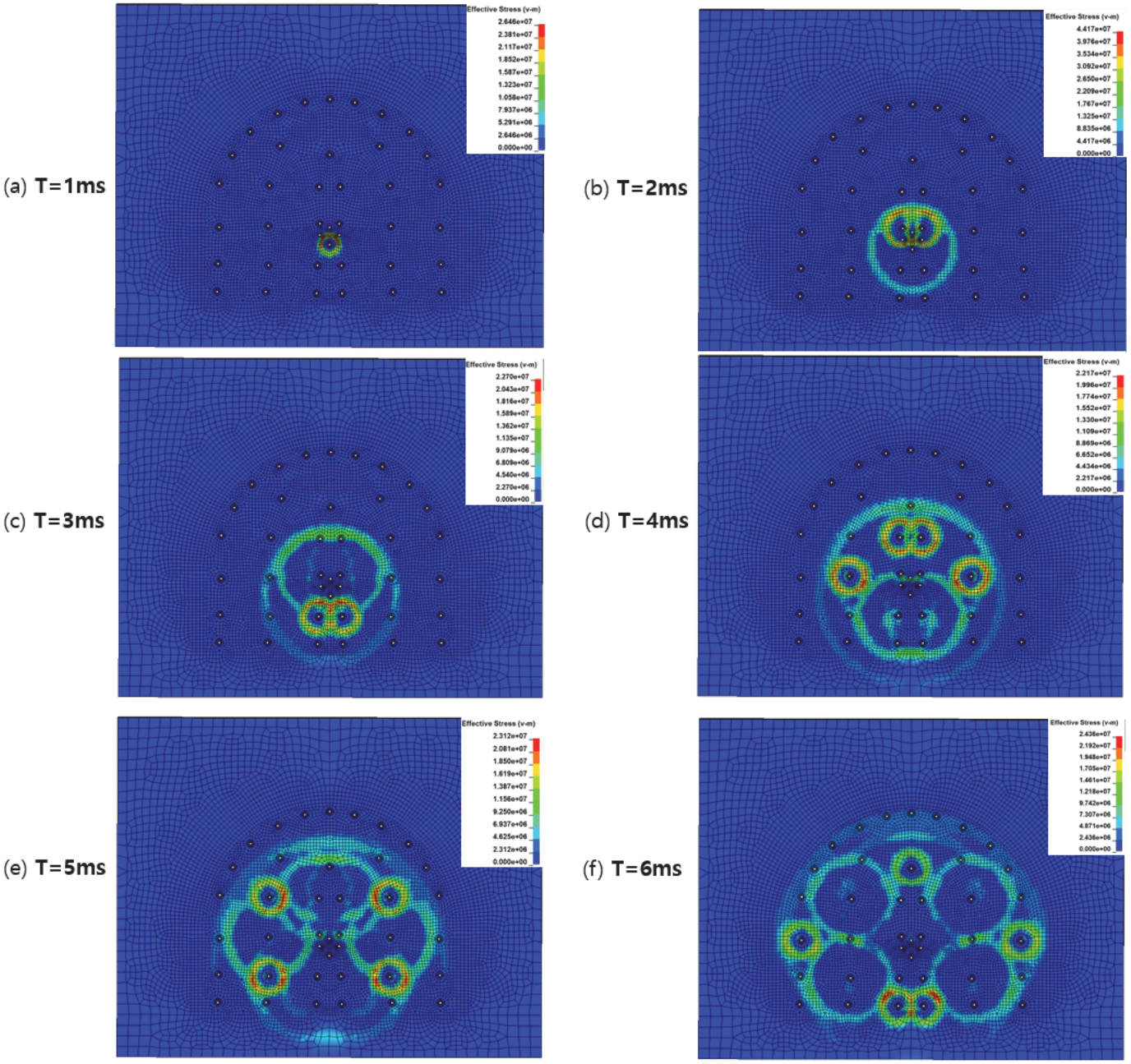

Figure 5: The effective stress propagation around explosive holes of tunnel blasting pattern based on delay time.

Parametric studies: acceleration parameter

The kinetic acceleration parameter was also investigated in addition to the velocity parameter, for the signaling elements. It reveals the impact of the load applied at these points. The acceleration response at the target points originating from the explosion charge reveals the characteristics including a high amplitude, short duration, and rapid reduction under the blast waves (Fig. 8). As seen in Fig. 8. a-e, the peak acceleration at Point B1 reaches 11,953 m/s² in 8.7 ms, which has the highest value compared to other points. The acceleration at Point A1 reaches 7933 m/s2 with the reduction of 34% to, at Point C1 it is 7786 m/s² with the reduction of 35% to, it is 5758 m/s² by the reduction of 52% at Point D1 and it reaches 7248 m/s² at Point E1 by the reduction of 40%. The results revealed that in range 2, there is a sharp reduction in acceleration movement compared to range 1. This acceleration rate is then relatively stable and not much different from other points. Acceleration decreases from 7933m/s² at Point A1 to 2750 m/s² at Point A5.

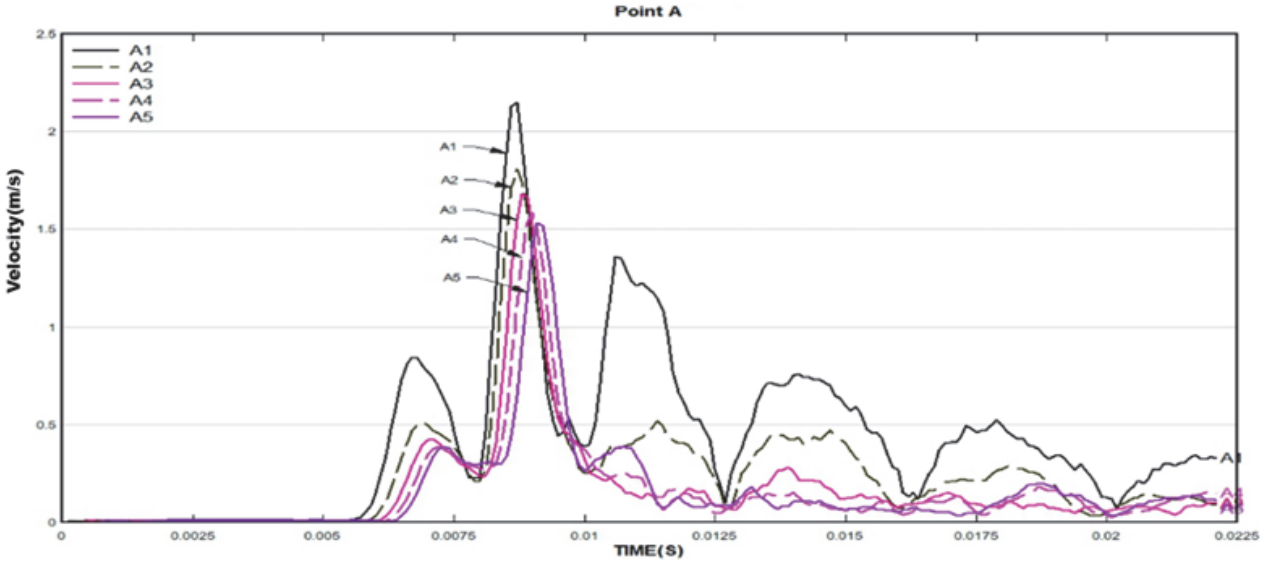
Point A
A1
A2
A3
A4
A5
Velocity(m/s)
TIME(S)

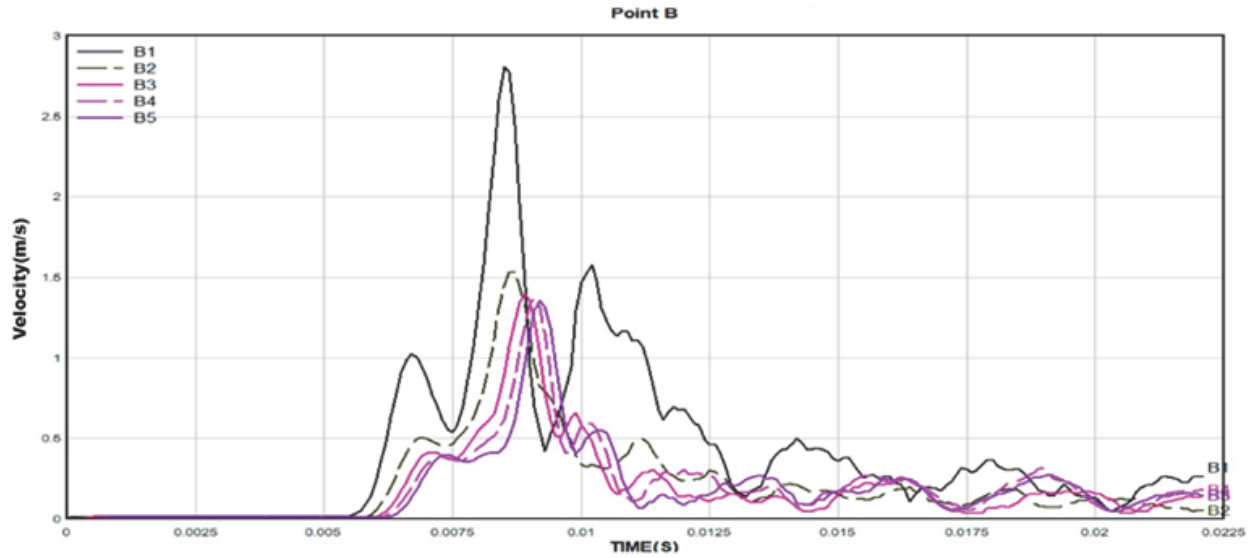
Point B
B1
B2
B3
B4
B5
Velocity(m/s)
TIME(S)

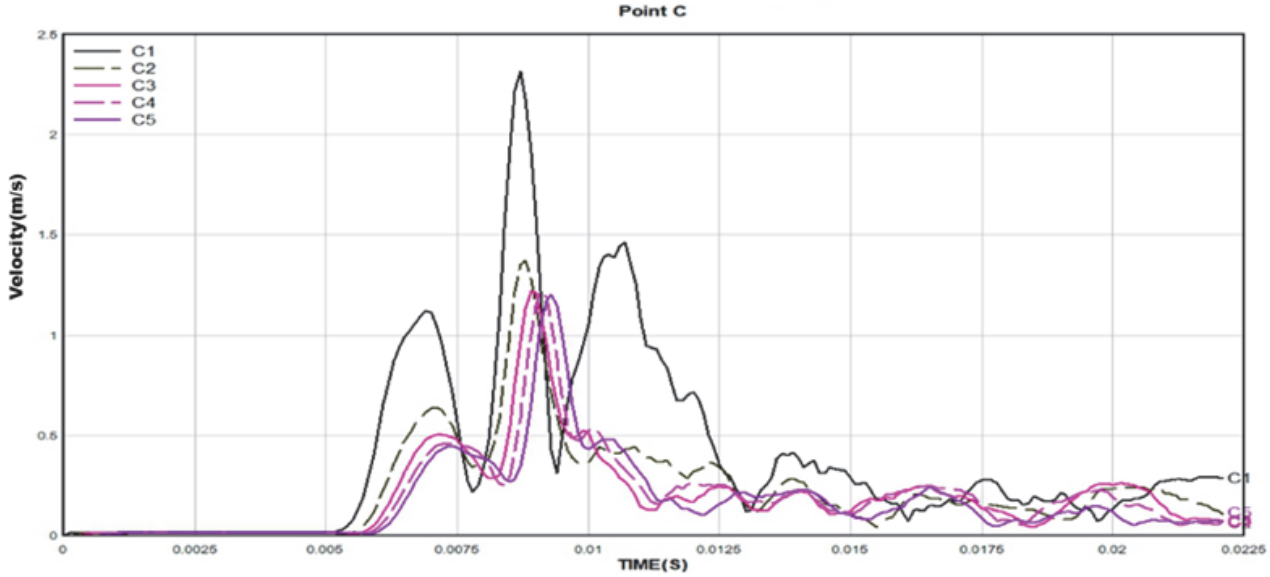
Point C
C1
C2
C3
C4
C5
Velocity(m/s)
TIME(S)

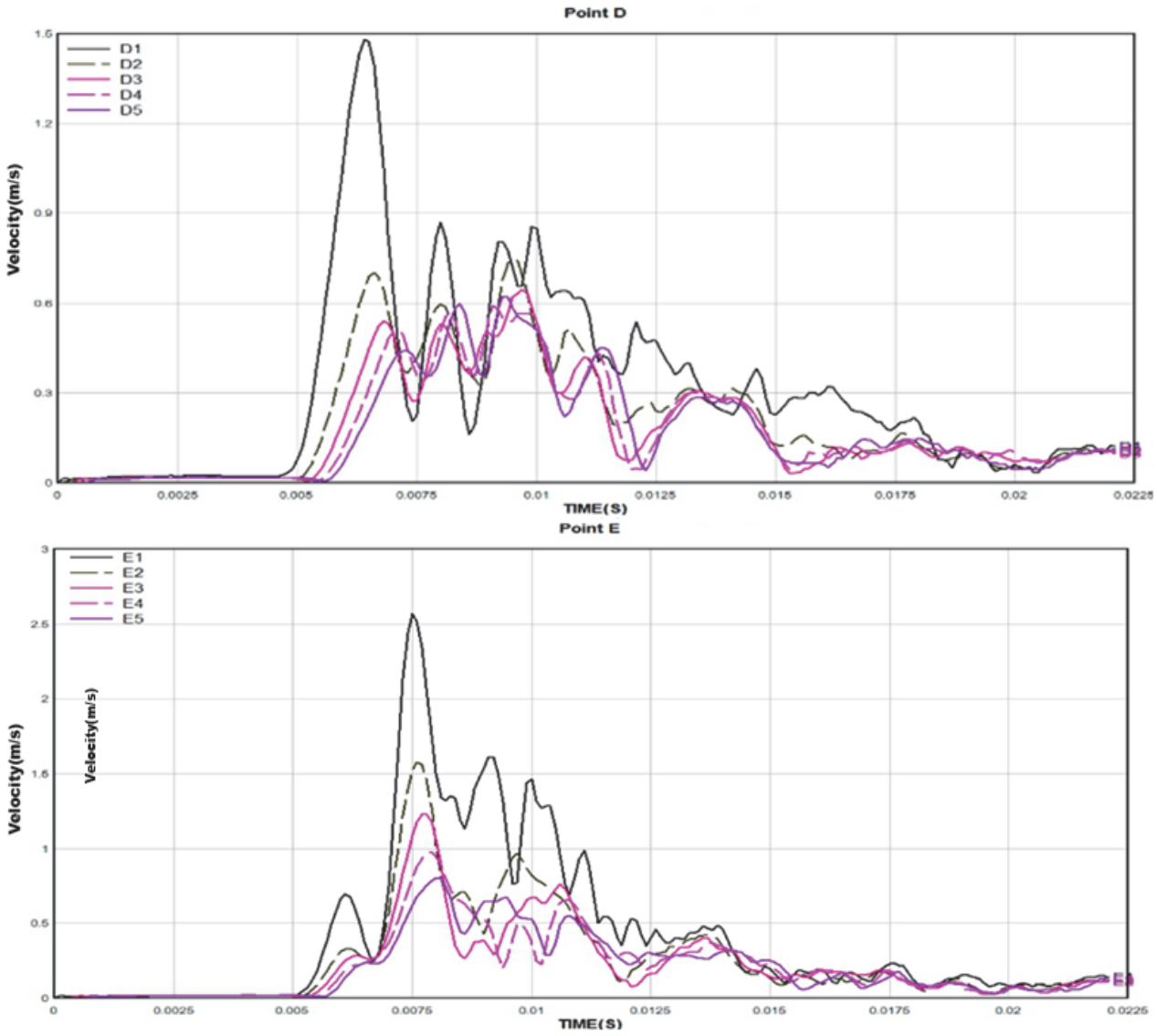

Figure 6: The chart of velocity history at sign points (a) Point A, (b) Point B, (c) Point C, (d) Point D, and (e) Point E.

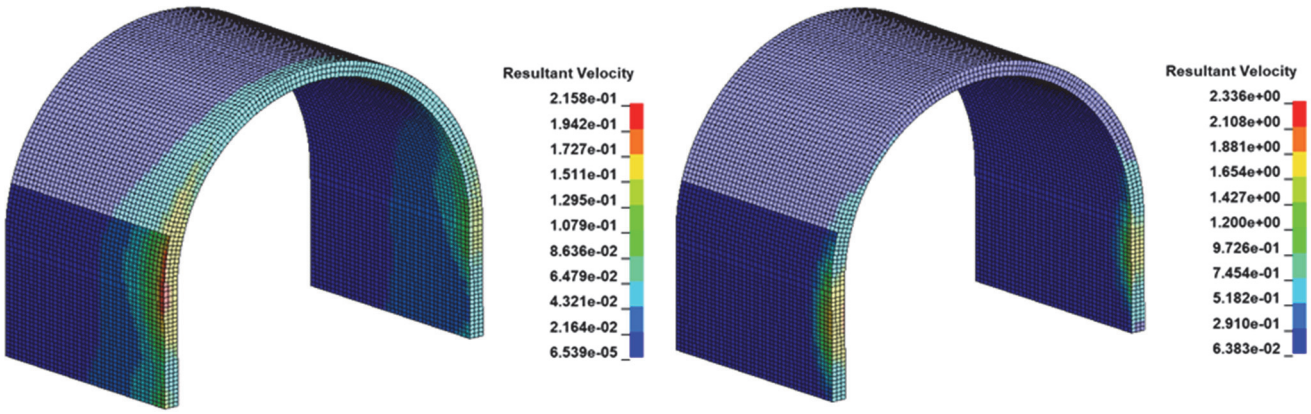

Figure 7: The velocity propagation contour in the elements of the tunnel support structure during blast.

At point B1, the acceleration is 11,953 m/s², which is the peak acceleration of the tunnel structure. It is 2700 m/s² at point B5. The peak acceleration reaches 2220, 1250, and 2350 m/s² at points C5, D5, and E5, with a reduction of 72%, 79% , and 68%, respectively. Similar to the graphs of velocity generated in the element, the first values of acceleration in the element occur in about 6 ms, which is small. This indicates the arrival of the blast wave of the intermediate holes exploded in less than 6 ms. However, the peak acceleration values occur at about 8 ms, after the seventh explosion, which is closest to the location of the elements with the highest volume of explosives.

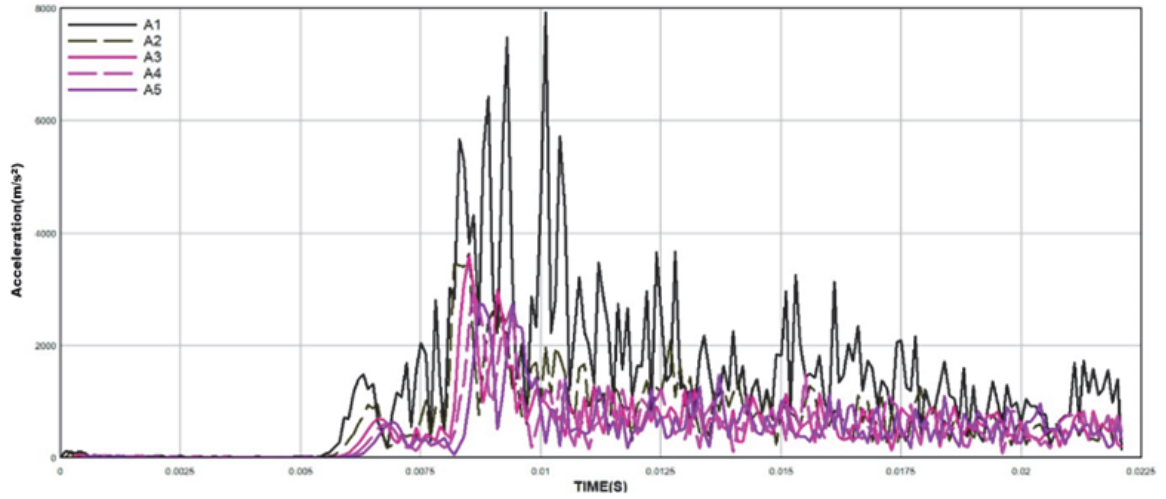

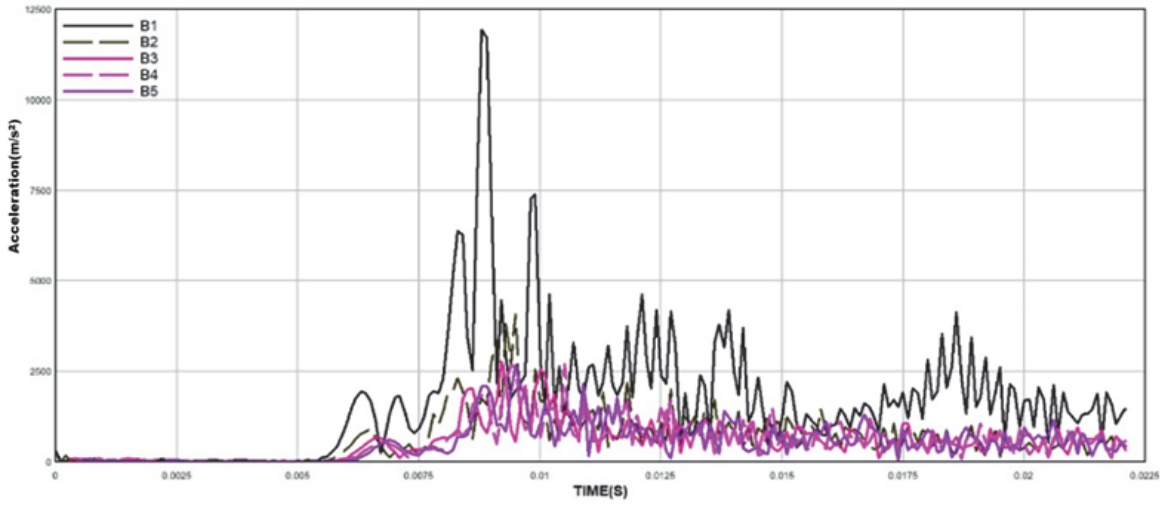

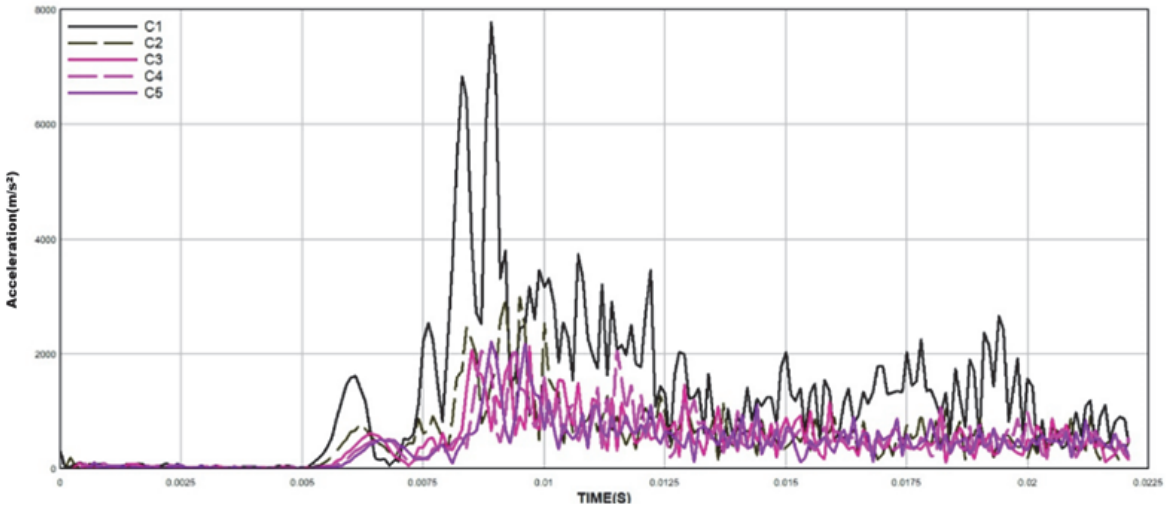

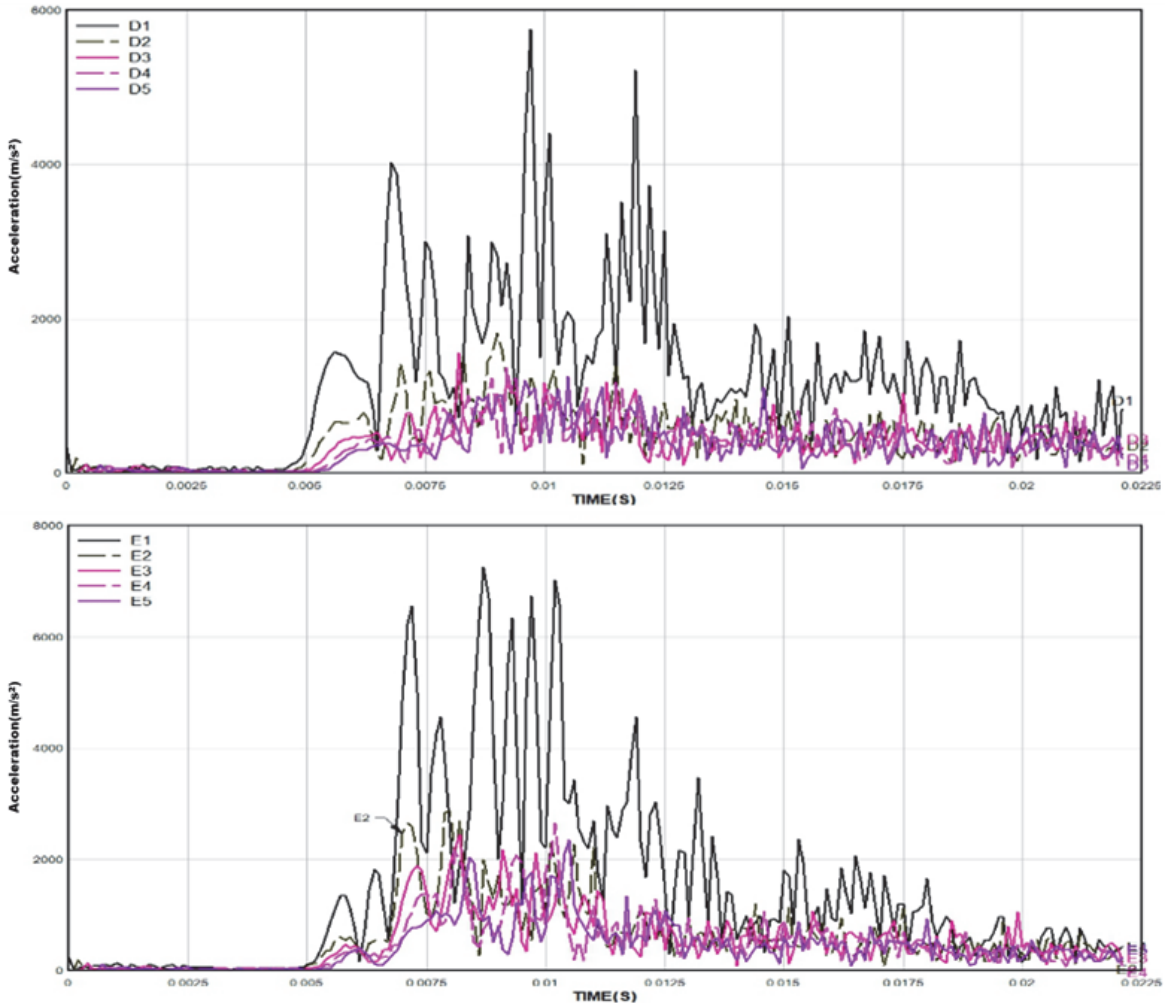

Figure 8: The diagram of acceleration time history at sign points of (a) Point A, (b) Point B, (c) Point C, (d) Point D, and (e) Point E.

Parametric studies: Safety assessment

To determine the reliability, the damage criterion was adopted using the peak particle velocity (PPV) method to assess the damage level of this underground tunnel. Brittle failure may occur when the stress in the tunnel wall reaches the rock mass resistance under the blast wave.[25] It is generally very difficult to obtain an accepted criterion of injury since it includes numerous factors. Generally, the level of damage caused by an explosion is based on numerous parameters, including the amount of explosive, the shape of the load, the depth of the explosion, and the type and characteristics of the soil. There are some experimental velocity criteria to investigate the possible failure of the underground structure. Hendron (1977) collected data on US military explosions nearby the tunnels in the sandstone environment. It was found that no damage occurred in the tunnels until the velocity exceeded 0.9 m/s. In this report, the damage was classified into four groups non-permanent failure, local failure, general failure, and severe failure. Tab. 7 presents different tunnel velocity damage criteria for various case studies [25]. Thus, considering the interaction and adhesion between the rock and the tunnel support structure, the failure level that achieved by the velocity of > 0.9 m/s² created in the elements of the tunnel support structure according to the Tab. 7 [4].

It can be seen in Tab. 8 that the rate of velocity created in the element is divided into three groups. The first category is the range of destruction level 2, the second category is in the range of destruction level 3, and the third category includes the elements with a velocity < 0.9 m/s. For the velocity of > 1.8 m/s, points A1, A2, B1, C1, and E1 fall in the first category. In this class, the compact spread in their lining while they are integrated under high compressive and tensile stresses. Then, the intact lining is divided into block structures. As a result, the overall stability fails and a damaged zone is developed, leading to the destruction of the affected areas.

In the area beyond the blast site, a generally damaged area was made for Points A3, A4, A5, B2-B5, C2-C5 Point D1, and E2 to E4 where the cracks thoroughly spread. Moreover, instability in the tunnel support structure is mainly related to its arch, which is vulnerable. The least damage is related to the points in the third category, i.e., the elements with a velocity of < 0.9 m/s. This includes Points E5 and D2-D5 representing the sidewall of the tunnel support structure. At these points, no destruction occurs in the tunnel support structure under blasting the working face.

PPV(m/s)	Damage	Damage Zone
NA	Tight closure	1
12	General failure (GF)	2
4	Local failure (LF)	3
0.9-1.8	Intermittent failure (IF)	4
0-0.9	No failure (NF)	5

Table 7: The type of structural damage based on the peak velocity [4].

	Range				
Point	1	2	3	4	5
A	LF	LF	IF	IF	IF
B	LF	IF	IF	IF	IF
C	LF	IF	IF	IF	IF
D	IF	NF	NF	NF	NF
E	LF	IF	IF	IF	NF

Table 8: The destruction level in the studied areas.

CONCLUSIONS

In this study, numerical modeling was done to simulate the behavior of the shotcrete together with lattice girder support as an equivalent cross-section under blasting loads in the rock media of the tunnel. Overall, the main results of this study can be outlined as follows:

• The peak particle velocity (PPV) criterion was used to assess tunnel safety under dynamic loads. Some elements failure levels occurred when the element's induced velocity exceeded 0.9 m/s. Investigating the elements of the temporary support structure of the tunnel indicated that this structure is damaged near the tunnel face to a distance of 2 m.

• The results obtained from investigating the equivalent cross-section of the tunnel support showed that:

1. The PPV created in the temporary tunnel support structure is related to Point B1, with a velocity of 2.9 m/s. According to the safety assessment of the tunnel, a local failure is possible at this point, which requires the reinforcement of the section or using an alternative blasting pattern with a less explosive load.
2. The tunnel structure at the distance of 2 m from the blast site is more vulnerable compared to the subsequent distances. Also, it will be damaged and cracked in Points A and B. Therefore, it is proposed to increase the cross-sectional thickness of the tunnel support structure in this section, especially in the tunnel crown.
3. There is an evident proportionality between the measured parameters of velocity, displacement, acceleration, and effective stress. These parameters are reduced based on the distance from the blast site and the blast wave attenuation in the tunnel support structure.
4. The results underline the importance of the structural response to the first blast wave originated from the explosion load in the elements with the peak value.

DATA AVAILABILITY STATEMENT

Some of all data, models, or codes that support the findings of this study are available from the corresponding author upon reasonable request.

REFERENCES

[1] Zhao, J., Zhou, Y. X., Hefny, A. M., Cai, J. G., Chen, S. G., Li, H. B. (1999). Rock dynamics research related to cavern development for ammunition storage. Tunnelling and Underground Space Technology, 14(4), pp. 513–526.

[2] Wu, C., Lu, Y. and Hao, H. 2004. Numerical prediction of blast-induced stress wave from large-scale underground explosion. International Journal for Numerical and Analytical Methods in Geomechanics, 28(1), pp. 93–109. DOI: 10.1002/nag.328.

[3] Luo, K.S., Wang, Y., Zhang, Y.T. and Huang, L.K., (2007). Numerical simulation of section subway tunnel under surface explosion. J. PLA Univ. Sci. Technol. (Nat. Sci. Ed.), 8(6), pp. 674-679.

[4] Mobaraki, B. and Vaghefi, M. 2015. Numerical study of the depth and cross-sectional shape of tunnel under surface explosion. Tunnelling and Underground Space Technology, 47, pp, 114–122. DOI: 10.1016/j.tust.2015.01.003.

[5] Mussa, M. H., Mutalib, A. A., Hamid, R. and Raman, S. N. (2018). Blast damage assessment of symmetrical box-shaped underground tunnel according to peak particle velocity (PPV) and single degree of freedom (SDOF) criteria. Symmetry, 10(5), pp. 158. DOI: 10.3390/sym10050158.

[6] Wang, J., Yin, Y. and Luo, C. (2018). Johnson–Holmquist-II (JH-2) constitutive model for rock materials: parameter determination and application in tunnel smooth blasting. Applied Sciences, 8(9), pp. 1675. DOI: 10.3390/app8091675.

[7] Jiang, N., Gao, T., Zhou, C. and Luo, X. (2018). Effect of excavation blasting vibration on adjacent buried gas pipeline in a metro tunnel. Tunnelling and underground space technology, 81, pp. 590-601. DOI: 10.1016/j.tust.2018.08.022.

[8] Li, Z., Wu, S., Cheng, Z. and Jiang, Y. (2018). Numerical Investigation of the Dynamic Responses and Damage of Linings Subjected to Violent Gas Explosions inside Highway Tunnels. Shock and Vibration. DOI: 10.1155/2018/2792043.

[9] Sharafisafa, M., Aliabadian, Z., Alizadeh, R. and Mortazavi, A. (2014). Distinct element modelling of fracture plan control in continuum and jointed rock mass in presplitting method of surface mining. International Journal of Mining Science and Technology. 24 (6). pp. 871- 881.

[10] Yang, J., Lu, W., Hu, Y., Chen, M. and Yan, P. (2015). Numerical Simulation of Rock Mass Damage Evolution During Deep-Buried Tunnel Excavation by Drill and Blast. Rock Mechanics and Rock Engineering,48(5), pp.2045–2059. DOI: 10.1007/s00603-014-0663-0.

[11] Zhao, H., Long, Y., Li, X. and Lu, L. (2016). Experimental and numerical investigation of the effect of blast-induced vibration from adjacent tunnel on existing tunnel. KSCE Journal of Civil Engineering, 20(1), pp. 431–439. DOI: 10.1007/s12205-015-0130-9.

[12] Ozacar, V. (2018). New methodology to prevent blasting damages for shallow tunnel. Geomechanics and Engineering, 15(6), pp. 1227–1236. DOI: 10.12989/GAE.2018.15.6.1227.

[13] Liu, F., Silva, J., Yang, S., Lv, H. and Zhang, J. 2019. Influence of explosives distribution on coal fragmentation in top-coal caving mining. Geomechanics and Engineering, 18(2), pp. 111-119. DOI: 10.12989/gae.2019.18.2.111.

[14] Guan, X., Zhang, L., Wang, Y., Fu, H. and An, J. (2020). Velocity and stress response and damage mechanism of three types pipelines subjected to highway tunnel blasting vibration. Engineering Failure Analysis, 118, p, 104840. DOI: 10.1016/j.engfailanal.2020.104840.

[15] Chamanzad, M. A. and Nikkhah, M. (2020). Sensitivity Analysis of Stress and Cracking in Rock Mass Blasting using Numerical Modelling. Journal of Mining and Environment, 11(4), pp. 1141-1155.

[16] Dimitraki, L., Christaras, B. and Arampelos, N. (2021). Investigation of blasting impact on limestone of varying quality using FEA. Geomechanics and Engineering, 25(2), pp. 111-121. DOI: 10.12989/gae.2021.25.2.111.

[17] Soleimani, S., (2016). Design of shotcrete support reinforced with lattice girder and analysis of geometric and strength properties effect of lattice in NATM tunnels (case study: Hakim tunnel). MSc thesis, Shahrood University of Technology, Shahrood, (Persian).

[18] Fu, J., Xie, J., Wang, S., Yang, J., Yang, F. and Pu, H. (2019). Cracking Performance of an Operational Tunnel Lining Due to Local Construction Defects. International Journal of Geomechanics, 19(4), pp. 04019019. DOI: 10.1061/(asce)gm.1943-622.0001371
[19] Cheng, D.S., Hung, C.W. and Pi, S.J. (2013). Numerical simulation of near-field explosion. Journal of Applied Science and Engineering , 16(1), pp. 61-67. DOI: 10.6180/jase.2013.16.1.09
[20] Hallquist, J. O. (2009). LS-DYNA KEYWORD USER'S MANUAL I, LSTC, Version, 971.
[21] Henrych, J. and Major, R. (1979). The dynamics of explosion and its use, 569. Elsevier Amsterdam.
[22] Jiang, N. and Zhou, C. (2012). Blasting vibration safety criterion for a tunnel liner structure. Tunnelling and Underground Space Technology, 32, pp. 52-57. DOI: 10.1016/j.tust.2012.04.016
[23] Jiang, Nan, and Chuanbo Zhou. (2012). Blasting vibration safety criterion for a tunnel liner structure. Tunnelling and Underground Space Technology, 32, pp. 52-57.
[24] Li, J. C., Li, H. B., Ma, G. W. and Zhou, Y. X. (2013). Assessment of underground tunnel stability to adjacent tunnel explosion. Tunnelling and Underground Space Technology, 35, pp. 227–234. DOI: 10.1016/j.tust.2012.07.005
[25] Hendron, A. J. (1977). Engineering of rock blasting on civil projects: Structural and Geotechnical Mechanics (Englewood Cliffs, NJ: Prentice-Hall), pp. 242–277, in International Journal of Rock Mechanics and Mining Sciences & Geomechanics Abstracts, (1978), 15(3), p. 66.